



Contents lists available at ScienceDirect

The Journal of Supercritical Fluids

journal homepage: www.elsevier.com/locate/supflu

Supercritical CO₂-assisted impregnation of LDPE/sepiolite nanocomposite films with insecticidal terpene ketones: Impregnation yield, crystallinity and mechanical properties assessment

María L. Goñi^{a,b}, Nicolás A. Gañán^{a,b,*}, Silvia E. Barbosa^c, Miriam C. Strumia^a,
Raquel E. Martini^{a,b}

^a IPQA, Universidad Nacional de Córdoba, CONICET, Av. Vélez Sarsfield 1611, X5016GCA, Córdoba, Argentina

^b Instituto de Ciencia y Tecnología de los Alimentos – ICTA (FCEFYN, Universidad Nacional de Córdoba), Av. Vélez Sarsfield 1611, X5016GCA, Córdoba, Argentina

^c Planta Piloto de Ingeniería Química, PLAPIQUI (UNS – CONICET), Departamento de Ingeniería Química, UNS, Camino La Carrindanga km. 7, 8000 Bahía Blanca, Argentina

ARTICLE INFO

Keywords:

Supercritical fluid impregnation
Terpene ketones
Sepiolite
Nanocomposites
Semicrystalline polymers

ABSTRACT

In this contribution, supercritical CO₂-assisted impregnation of LDPE/sepiolite nanocomposite films with two insecticidal terpene ketones (thymoquinone and *R*-(+)-pulegone) is investigated, as a strategy to enhance the loading capacity compared to pure LDPE. A factorial experimental design was applied in order to evaluate the effect of five process variables at two levels (sepiolite content: 1–10% w/w; initial ketone mole fraction: 0.0017–0.0025; pressure: 9–13 MPa; depressurization rate: 0.5–2.0 MPa/min; time: 2–4 h) on impregnation yield, at 45 °C. ANOVA test of the results indicated that pressure, time and ketone mole fraction significantly affect impregnation yield (ranging between 2.36 ± 0.18 and $8.60 \pm 1.66\%$ w/w). Thermal analysis (DSC) and X-ray diffraction (XRD) allowed to investigate the nanocomposite morphology and the modifications induced by the impregnation. The mechanical properties of the films were assessed by stress-strain tests, showing that the impregnation process had a very low impact on the material ductility and strength.

1. Introduction

Supercritical carbon dioxide (scCO₂) assisted impregnation of polymers with active compounds has been proposed and studied as an attractive technology for the development of active materials with potential applications in medicine, pharmacy, food packaging and pest control, among others [1–4], based on the well known properties of scCO₂ as “eco-friendly” solvent with tunable properties. In a typical process, the polymer (which may be in the form of films, pellets, fibers, etc.) is put in contact with a scCO₂ phase where the active substance to be loaded is dissolved. Under high pressure conditions, CO₂ is absorbed into the polymer, promoting its swelling and plasticization, and enhancing solute diffusion through the polymeric matrix by increasing the system free volume [1]. The sorption and swelling behavior of different polymer-scCO₂ systems and its dependence on pressure and temperature conditions have been studied by several authors [5–9]. After some contact time, the system is depressurized, CO₂ is desorbed, the polymer recovers (totally or partially) its original volume and morphology and the solute molecules are retained into the polymeric matrix to some extent. The final amount of solute loaded into the polymer depends on

thermodynamic as well as mass transfer factors. The maximum impregnation yield is determined by the solute partition coefficient between the polymer and the fluid phase, which depends on the system temperature, pressure and composition. Besides, as the solute diffusion into the polymer is the rate controlling step, a certain time of exposure is required in order to reach thermodynamic equilibrium. Mass transfer is highly dependent on concentration gradients and the physico-chemical properties of both the polymer and the fluid (mainly density and viscosity). The occurrence of specific or strong solute-polymer interactions (such as dipole–dipole or hydrogen bonding, hydrophilic or hydrophobic interactions) will enhance solute retention and therefore polymer loading [10].

Among the most promising applications, we can mention the scCO₂-assisted dying of polymers and textile fibers [11,12], the impregnation of contact lenses, implants and sutures with pharmacological compounds [13–15], the incorporation of antimicrobials in food packaging materials [16–18] and biopolymers [19–21], and the direct impregnation of wood with antifungal compounds [22], as some relevant examples. Some applications have successfully reached industrial scale, such as wood impregnation [23] and textile fibers dying [24].

* Corresponding author at: IPQA, Universidad Nacional de Córdoba, CONICET, Av. Vélez Sarsfield 1611, Córdoba, X5016GCA, Argentina.
E-mail address: nganan@plapiqui.edu.ar (N.A. Gañán).

<http://dx.doi.org/10.1016/j.supflu.2017.06.013>

Received 12 May 2017; Received in revised form 22 June 2017; Accepted 23 June 2017
0896-8446/ © 2017 Elsevier B.V. All rights reserved.

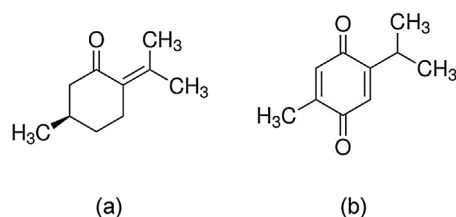


Fig. 1. Chemical structures of terpene ketones: (a) R-(+)-pulegone and (b) thymoquinone.

Particularly in our group, an application currently investigated is the incorporation of biopesticides into polymeric films commonly used for food packaging or crop protection, with the objective of controlling insect pests during storage or transport. In a previous work [25], we have studied the scCO₂-assisted impregnation of low-density polyethylene (LDPE) films with a mixture of two selected terpene ketones (pulegone and thymoquinone) with insecticidal activity against the corn weevil (*Sitophilus zeamais*) [26]. The chemical structure of these terpene ketones is shown in Fig. 1. Film samples were impregnated under different combinations of pressure, ketone mole fraction, contact time and depressurization conditions, in order to investigate the effect of these variables on the impregnation efficiency. The ketone content in the impregnated films ranged between 2 and 6% (w/w), and their fumigant toxicity against *S. zeamais* was confirmed and evaluated in laboratory bioassays [25,27].

The aim of this work is to explore the application of scCO₂-assisted impregnation for the incorporation of this mixture of terpene ketones into LDPE/sepiolite nanocomposite films. Polymer/clay composites have been studied as suitable carrier and packaging materials for the controlled release of active substances [28], as a result of the adsorption of solute molecules onto the dispersed clay nanoparticles. Besides release control, the adsorption onto the porous structure of nanoclays also preserves active compounds from degradation due to sunlight irradiation, temperature, oxygen and reduces losses by leaching or excessive evaporation, for example in the case of pesticides [29]. Therefore, the use of a LDPE/sepiolite nanocomposite as impregnation matrix is presented as a potential strategy for enhancing the loading capacity as well as the final properties with respect to pure LDPE films.

Sepiolite is a hydrated magnesium silicate clay whose half-unit formula is Si₁₂O₃₀Mg₈(OH,F)₄(OH₂)₄·8H₂O. Its structure consists of talc type sheets, i.e., planes formed by an octahedral layer (Mg) between two external tetrahedral layers (Si), and these sheets are separated by so-called zeolitic channels, characterized by the presence of water molecules, as can be seen in Fig. 2 [30]. The particular arrangement of

atoms produces a needle-like (acicular) structure, instead of typical plate-like one. For this reason sepiolite has one of the highest surface area of all clay minerals: about 300 m²/g [31]. Their particles are arranged forming loosely packed and porous aggregates with an extensive capillary network which explains the high porosity and light weight because of the high void space fraction. The high surface area and porosity account for the remarkable adsorptive and absorptive properties of this clay: it adsorbs vapor and odors and can absorb approximately its own weight of water and other liquids [31]. The presence of a high number of silanol groups (Si–OH) exposed at the pores surface can interact with water and polar substances (such as ketones). Besides its excellent sorption properties, sepiolite also enhances the mechanical resistance and thermal stability of polymeric materials. Sepiolite and other related clays have been applied as nanofillers in the development of active films and coatings loaded with essential oils and related volatile compounds. For example, Tornuk et al. have reported the incorporation of nanoclays grafted with thymol, eugenol and carvacrol to LDPE films for meat products preservation [32], while Gimenez et al. have investigated the dispersion of sepiolite in gelatin-egg white films for the controlled release of clove oil as antioxidant and antimicrobial agent [33]. Chevillard et al. have studied the role of different montmorillonites in modulating the diffusion rate of a model pesticide in wheat gluten-based polymers [34]. In these applications, the active substance is generally adsorbed onto the nanofiller before its dispersion into the polymeric matrix, or added directly to the molten polymer (or polymer solution) before film casting. However, to the best of our knowledge, the direct impregnation of LDPE/clay type nanocomposite films by scCO₂-assisted impregnation has not been previously reported in the literature.

In this study, the effect of the main process variables (impregnation pressure, ketone mole fraction, contact time and depressurization rate), as well as the sepiolite content in the polymer, on the impregnation performance is investigated, using a factorial design of experiments (DOE). This approach allows a rapid screening and determination of the variables that affect significantly the process output [35] and provides useful information for further optimization purposes. The morphology of the nanocomposite matrix, as well as the modifications induced by the impregnation process, are investigated by thermal analysis and X-ray diffraction (XRD). Finally, the mechanical performance of the impregnated material is assessed.

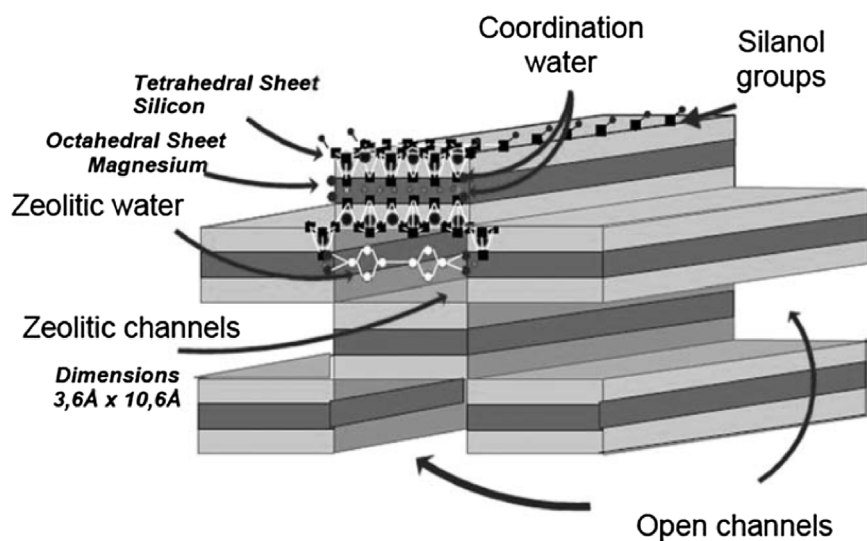


Fig. 2. Scheme of sepiolite structure [30].

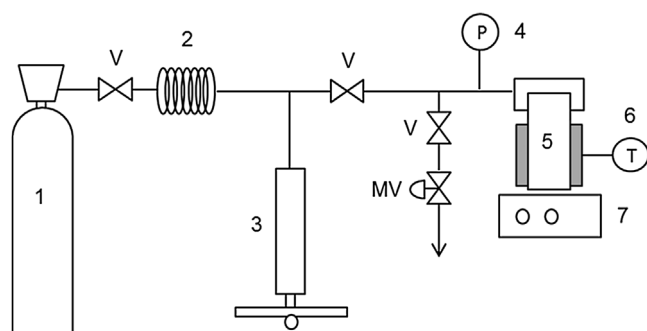


Fig. 3. High pressure impregnation apparatus. 1, CO₂ reservoir; 2, cooling coil; 3, pressure generator; 4, manometer; 5, impregnation cell; 6, temperature controller; 7, magnetic stirrer; V, valves; MV, micrometering valve.

2. Materials and methods

2.1. Materials

R-(+)-pulegone ($\geq 97\%$, MW: 152.2 g/mol, bp: 224 °C) and thymoquinone ($\geq 99\%$, MW: 164.2 g/mol, mp: 45 °C) were purchased from Sigma-Aldrich (Steinheim, Germany). Industrial extra-dry carbon dioxide (water content ≤ 10 ppm v/v, Linde, Argentina) was used as impregnation solvent.

The nanocomposite films were prepared using low-density polyethylene (LDPE, Dowlex 2045, Dow Chemical) and sepiolite (PRG4, Tolsa, Spain) as nanofiller, according to the procedure described by Martini et al. [30]. Films with 1 and 10% w/w of sepiolite and 27 ± 3 μm thickness were used for impregnation. More details about the synthesis procedure and film characterization can be found in the cited work [30].

2.2. Impregnation equipment and method

Impregnation experiments were performed in a lab-scale high pressure system schematically represented in Fig. 3. The impregnation chamber consists of a 50 cm³ stainless steel cell (2 cm internal diameter) which can operate up to 25 MPa and 200 °C. It is externally heated by an aluminium jacket and a resistance clamp connected to a temperature controller (Instrelec, Argentina). Agitation is provided by a magnetic stirrer (Arcano, Argentina), using a small magnet coated with teflon placed into the cell. A metal mesh support is used to maintain the films inside the cell in a vertical position, in order to minimize the deposition of ketone droplets on the film surface during depressurization. This metal support also prevents the films from sticking together, which ensures impregnation through both sides of the films. First, the cell is loaded with a certain amount of an equimolar mixture of both terpene ketones – depending on the operation conditions– and the nanocomposite films are placed into the cell using the metal support. In this work, film samples with 50–100 mg weight were used, with approximate surface area of 10–20 cm². Immediately after loading, the cell is closed, the heating resistance activated, and liquid CO₂ is delivered to the cell using a pressure generator (HiP, USA) or a hand pump, until the system is equilibrated at the desired values of pressure and temperature, performing minor pressure corrections when necessary, until reaching steady conditions. The CO₂ is previously liquefied in a 2 °C water cooling bath (Lauda, Germany).

Afterwards, the impregnation experiment proceeds at constant pressure, temperature and agitation rate for a certain period of time, and then the heating and stirring systems are turned off and the cell is depressurized under controlled conditions at constant rate, by means of a micrometering valve (Swagelok, USA). The outlet line and the valve are wrapped with a heating tape in order to avoid the formation of solid particles due to the cooling effect of CO₂ expansion, which may affect the depressurization rate control. After depressurization, the cell is

opened and the films are carefully removed and cleaned superficially with tissue paper in order to eliminate ketone droplets.

The mass of ketones incorporated into the films was determined gravimetrically in a precision balance and the impregnation yield (Y%) was calculated according to Eq. (1):

$$Y\% = \frac{m_f - m_o}{m_o} \times 100 \quad (1)$$

where m_o and m_f are the original and the final mass of the film, before and after impregnation, respectively. In order to ensure the complete release of dissolved CO₂ from the films after depressurization, which can affect the gravimetric measurements, the samples were weighed at least 10 min after depressurization [25]. Preliminary runs were performed without the addition of ketones, and no change in the films weight was observed after treatment, indicating that CO₂ is desorbed rapidly from the films. These tests also allowed to confirm that extraction of sepiolite or polymer additives by scCO₂ does not occur under the studied conditions.

2.3. Experimental design

A 16-run standard fractional factorial design of experiments was applied in order to assess the effect of five selected factors at two levels: (A) sepiolite content, (B) ketone mole fraction, (C) pressure, (D) depressurization rate, and (E) contact time. This arrangement allows to estimate all main factor effects and two-factor interactions aliased only by three-factor or higher order interactions [36]. The corresponding high and low values are presented in Table 1. All impregnation runs were performed at the same temperature (45 °C). This value was selected based on our own previous works [18,25], as well as works of other authors [16,17], to facilitate comparison. Besides, this temperature was considered low enough to preserve these thermolabile natural compounds, but far enough from the critical temperature to avoid density fluctuations (and to allow a better control). As previously mentioned, films with 1 and 10% (w/w) sepiolite were used as impregnation matrix. Factor B corresponds to the initial mole fraction of the equimolar mixture of ketones in the fluid phase. For all runs the cell was loaded with a ketone/CO₂ molar ratio below the solubility value, in order to ensure a total solubilization of both ketones at all tested pressures. As CO₂ density changes with pressure and the cell volume is fixed, different amounts of ketones had to be loaded according to the pressure level. When using this approach, it has to be noted that ketone mole fraction in the fluid phase decreases as the impregnation proceeds. Although this is not convenient from the point of view of the mass transfer process (compared to using an excess amount of ketones), it allows to assess separately the effect of concentration and pressure. Pressure values were selected in order to cover a broad range of CO₂ densities (337 and 694 kg/m³, at 45 °C and 9 and 13 MPa, respectively). Slow (0.5 MPa/min) and fast (2 MPa/min) depressurization conditions were compared. Finally, contact time values (2 and 4 h) were determined based on our own previous works [18,25], as well as information reported by other authors for similar systems [16,17].

The total amount of ketones incorporated into the LDPE films per unit weight of material (impregnation yield) was evaluated as the process response, and the effect of each factor and all two-factor interactions on this response was statistically determined by analysis of

Table 1
Experimental variables for two-level factorial design.

Factor	Variable	Low level (–)	High level (+)
A	Sepiolite% (w/w)	1	10
B	Initial ketone mole fraction	0.0017	0.0025
C	Pressure (MPa)	9	13
D	Depressurization rate (MPa/min)	0.5	2
E	Time (h)	2	4

variance (ANOVA) using the software Statgraphics® (StatPoint Technologies, Inc.) [35]. Effects were considered significant for $p < 0.05$.

2.4. Fourier transformed infra-red spectrometric analysis (FTIR)

The impregnated films were analyzed by Fourier transformed infrared (FTIR) spectrometry in order to confirm the incorporation of ketones. Absorbance spectra were obtained in an infrared imaging microscope (Nicolet iN10 Mx, Thermo Fisher Scientific, USA), with a resolution of 2 cm^{-1} , in a wavenumber range of $400\text{--}4000\text{ cm}^{-1}$ with 16 scans, at room temperature. Spectra of the pure ketones, original LDPE/sepiolite film and impregnated film samples were acquired and compared in order to identify characteristic absorbance bands. Pure thymoquinone and *R*-(+)-pulegone were dissolved in paraffin oil, in order to obtain a molecular environment similar to polyethylene [37]. Background spectra were acquired before each test for air humidity and carbon dioxide correction.

2.5. Thermal analysis

Thermal properties were analyzed by differential scanning calorimetry (DSC) in a Discovery DSC (TA Instruments, USA). Thermograms were obtained directly on film samples heating from $25\text{ }^{\circ}\text{C}$ to $180\text{ }^{\circ}\text{C}$ and cooling from $180\text{ }^{\circ}\text{C}$ to $25\text{ }^{\circ}\text{C}$, at $10\text{ }^{\circ}\text{C}/\text{min}$, at ambient pressure and under nitrogen atmosphere. Impregnated as well as untreated film samples were analyzed in order to evaluate possible effects of the impregnation process on the material properties. Melting temperatures and enthalpies from the first heating cycle were recorded, and the crystallinity degree was calculated by comparison with the melting enthalpy of pure crystalline LDPE.

2.6. X-ray diffraction (XRD) analysis

Crystal orientation was analyzed by XRD in a Philips PW 1710 diffractometer, with a graphite curve monochromator, Cu anode, 45 kV, and 30 mA. Two different experiments were performed varying the film stretching direction respect to the X-ray beam (parallel and perpendicular). In order to verify the repeatability of the data, five spectra for each sample were performed.

2.7. Mechanical properties

Tensile strength tests were performed using a universal testing machine (Instron, USA) in order to determine the effect of the high pressure impregnation on the mechanical properties of the nanocomposite films. For this purpose, impregnated, pressurized (only with scCO_2) and untreated film samples were tested and compared. Similar rectangular probes ($50 \times 10\text{ mm}$) were used in all runs, with an initial grip separation of 30 mm. Tests were conducted under a constant cross-head speed of $100\text{ mm}/\text{min}$ until break. Young modulus, yield strength, tensile strength and elongation at break were recorded along each test. The films thickness was measured prior to all tests with a precision micrometer (Wembley, China). All tests were replicated at least five times.

3. Results and discussion

3.1. ScCO_2 -assisted impregnation

Impregnation yield results obtained in all experimental runs at different operation conditions are shown in Table 2. In general, scCO_2 -assisted impregnation process was effective for the incorporation of ketones into the nanocomposite films, with final content ranging between 2.36 ± 0.18 and $8.60 \pm 1.66\%$ (w/w). These values are comparable with results reported by other authors for the impregnation

of polyethylene films with terpenes and other compounds with similar molecular weight and/or chemical structure, for example styrene [38], thymol [16] and 2-nonanone [17], as well as our own previous results using eugenol [18] and terpene ketones [25], within a similar range of operation conditions. In the last case, maximum yield obtained for pulegone and thymoquinone in pure LDPE films was 5.6% (w/w), suggesting that the presence of sepiolite as nanofiller enhanced the incorporation of ketones.

The impregnated films were analyzed by FTIR spectrometry, as described in Section 2.4, and the absorbance spectra were compared with the non-treated material and the pure ketones spectra in order to identify their characteristic bands. Fig. 4 shows an example of FTIR spectra for two films with 1 and 10% (w/w) sepiolite, before and after impregnation. Typical polyethylene (PE) absorption bands can be seen at approx. 715 , 1450 and $2800\text{--}3000\text{ cm}^{-1}$. The absorption bands in the $900\text{--}1100\text{ cm}^{-1}$ range correspond to Si–O bonds in the sepiolite particles [39], and consequently their intensity is higher in the 10% sample (B). The presence of ketones is generally indicated by an absorption band at $1660\text{--}1700\text{ cm}^{-1}$, typical of carbonyl (C=O) bonds. Although there are some weak bands in the $1600\text{--}1700\text{ cm}^{-1}$ region in the original film, corresponding to water molecules adsorbed onto the sepiolite pores (zeolitic water) [39], the appearance of a sharp band at $\sim 1680\text{ cm}^{-1}$ after impregnation can be clearly observed, which indicates the incorporation of ketones into the treated material.

A closer inspection of the FTIR spectra and a comparison with the pure ketones (dissolved in paraffin oil) allows the identification of both compounds in the impregnated material. As can be seen in Fig. 5 for a selected sample, thymoquinone shows a characteristic absorption band at 1238 cm^{-1} , typical of aromatic C=C bonds [40], while the band at 1208 cm^{-1} of *R*-(+)-pulegone can be assigned to the vibration of C–H bonds in the $>\text{CH}-\text{CH}_3$ group [41]. This last band is more clearly visible in the film samples with 1% sepiolite, but it is overlapped by other bands in the 10% sepiolite samples, as can be seen by comparing Figs. 4 and 5.

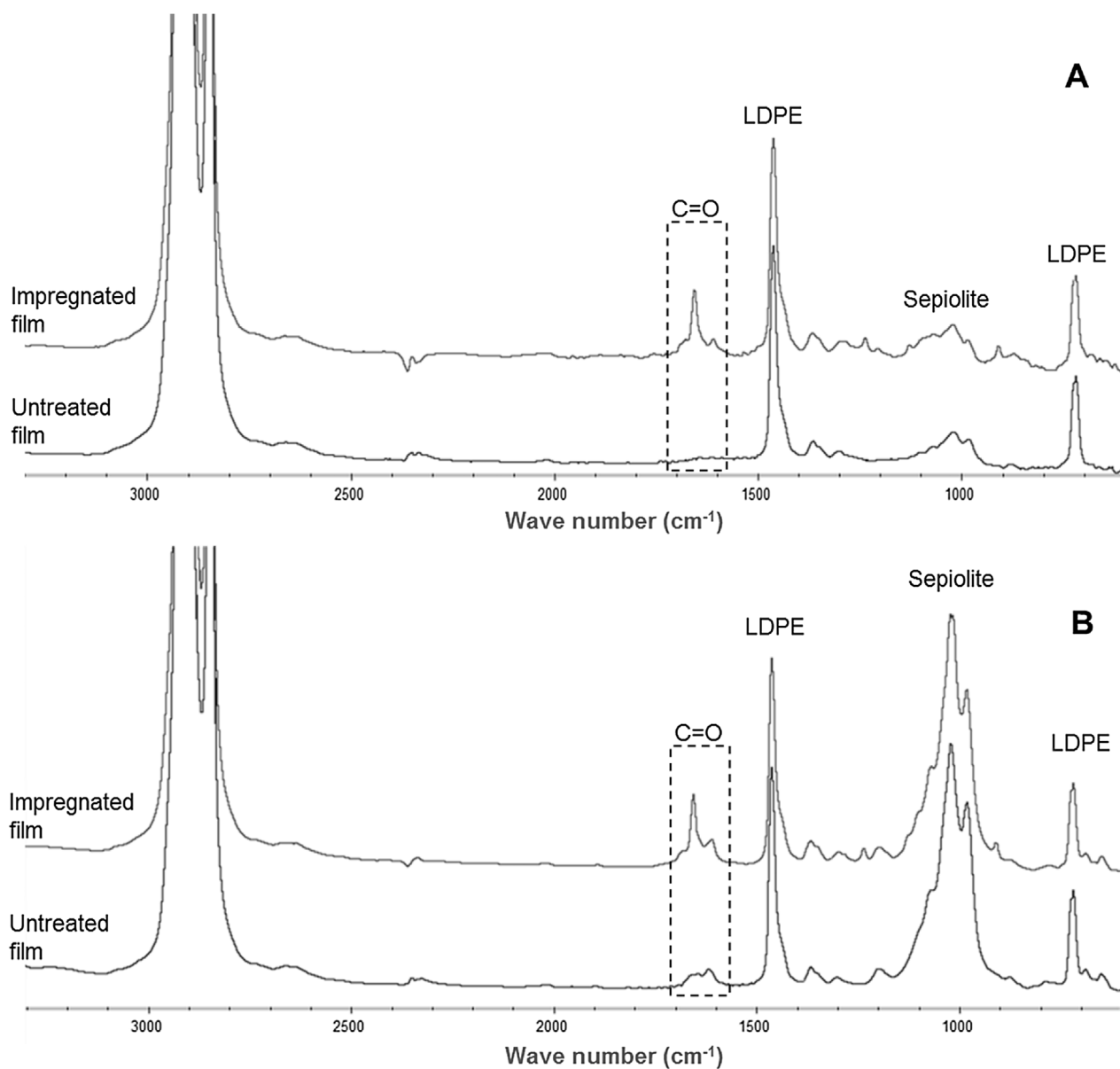
Table 3 shows the ANOVA test results for the experimental design, showing the calculated effect of each factor on the impregnation yield (Y%). As mentioned, effects were considered statistically significant for $p < 0.05$. The Pareto diagram presented in Fig. 6 shows the standardized effects in a graphical way. Results indicate that pressure (C), ketones mole fraction (B) and contact time (E) have significant effects on the impregnation process yield.

In the case of pressure, a negative effect is observed within the studied range. In other words, the mean yield value of all experiments performed at low pressure (9 MPa) was significantly higher than the mean yield value obtained operating at the high pressure level (13 MPa). Pressure has influence on the system thermodynamics as well as on transport properties. In fact, it has been shown that high pressure CO_2 sorption in polymers increases with pressure (at constant temperature) [42], which in turn enhances solute diffusivity in the polymeric matrix by increasing the free volume (swelling) and the polymer chains mobility (plasticization). At the same time, CO_2 density and solvent power increase with pressure, enhancing the affinity of the solutes for the fluid phase (which is usually evidenced by an increase of solute partition coefficients). The fluid viscosity also increases with pressure, which may have some impact on mass transfer rates. In the case of polymer/clay composites, pressure may have an additional effect on the solute adsorption equilibrium onto the porous particles surface. It has been demonstrated that the adsorption of terpenes and other natural compounds onto silica gel and other common adsorbents decreases with CO_2 density [43]; this effect has been proposed for the fractionation of mixtures using an adsorption/desorption cycle by simple pressure change [44].

The net result of these opposite effects on the solute–polymer–fluid system properties will depend on which one prevails at different pressure conditions. Some authors have observed the occurrence of an optimum at an intermediate pressure value where the impregnation yield

Table 2Experimental design for process conditions and impregnation yields obtained (Y%). All impregnation runs were performed at $T = 45\text{ }^{\circ}\text{C}$.

Run no.	Sepiolite (%)	Initial ketone mole fraction	Pressure (MPa)	Depressurization rate (MPa/min)	Time (h)	Y %
1	1	0.0017	9	0.5	4	2.81 ± 0.10
2	10	0.0017	9	0.5	2	3.72 ± 0.29
3	1	0.0025	9	0.5	2	7.45 ± 0.93
4	10	0.0025	9	0.5	4	8.60 ± 1.66
5	1	0.0017	13	0.5	2	2.71 ± 0.50
6	10	0.0017	13	0.5	4	5.06 ± 0.04
7	1	0.0025	13	0.5	4	2.79 ± 0.39
8	10	0.0025	13	0.5	2	2.45 ± 0.25
9	1	0.0017	9	2	2	5.35 ± 1.03
10	10	0.0017	9	2	4	4.60 ± 1.12
11	1	0.0025	9	2	4	6.03 ± 0.53
12	10	0.0025	9	2	2	2.99 ± 0.89
13	1	0.0017	13	2	4	2.68 ± 0.94
14	10	0.0017	13	2	2	3.86 ± 0.50
15	1	0.0025	13	2	2	2.36 ± 0.18
16	10	0.0025	13	2	4	4.42 ± 0.10

Mean values \pm standard deviation with $n = 2$.**Fig. 4.** FTIR spectra of untreated and impregnated LDPE/sepiolite nanocomposite films with 1% (A) and 10% (B) sepiolite content. (Impregnation conditions: $T = 45\text{ }^{\circ}\text{C}$; $P = 9\text{ MPa}$; depressurization rate = 0.5 MPa/min ; time = 4 h ; initial ketone mole fraction = 0.0025).

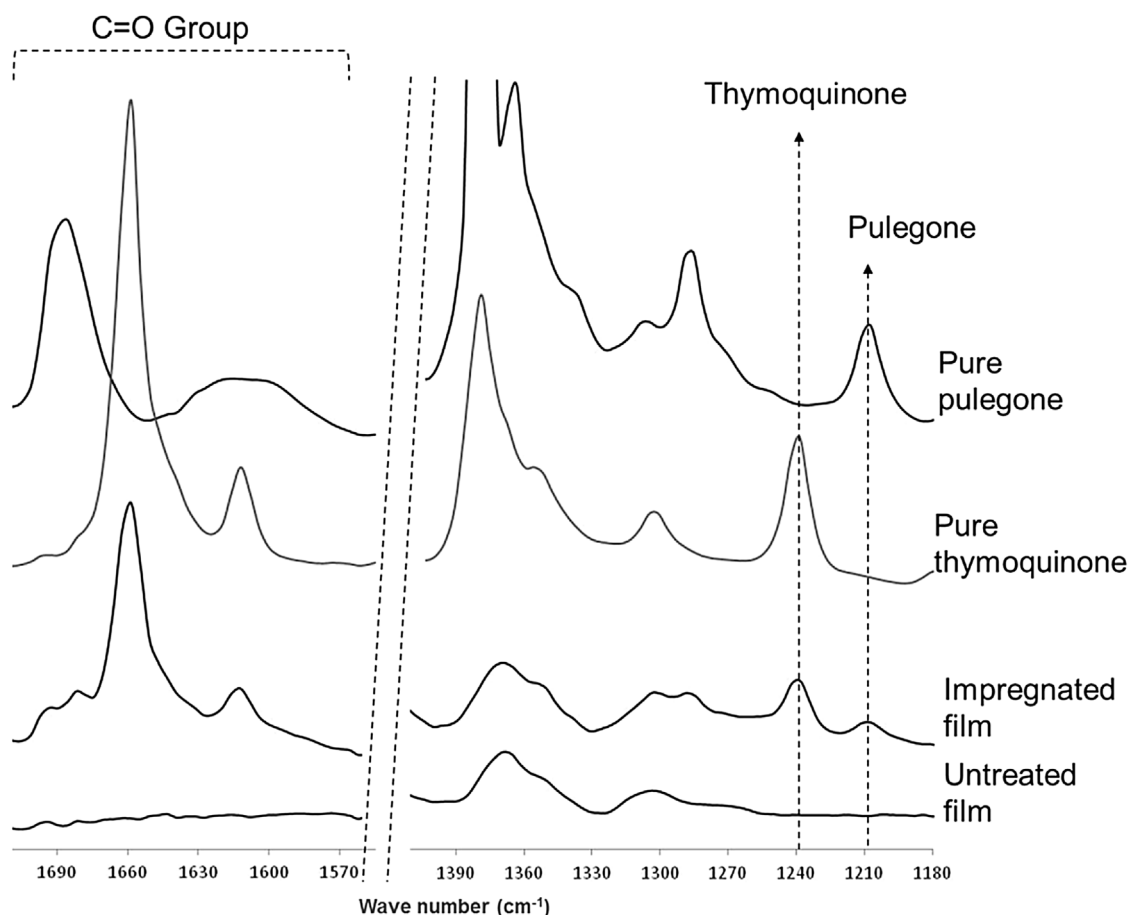


Fig. 5. Characteristic FTIR absorbance bands of thymoquinone and pulegone (pure and loaded into LDPE/sepiolite films). Impregnated film corresponds to run 4.

Table 3

ANOVA testing the effects of process variables on impregnation yield (Y%) for the fractional design model.

Factor	DF	Effect	SS	MS	F	p-value
A: Sepiolite%	1.00	0.44	1.54	1.54	2.82	0.113
B: Initial ketone mole fraction	1.00	0.79	4.95	4.95	9.05	0.008
C: Pressure	1.00	-1.90	28.96	28.96	52.99	< 0.001
D: Depressurization rate	1.00	-0.41	1.34	1.34	2.46	0.136
E: Time	1.00	0.76	4.65	4.65	8.51	0.010

DF: Degrees of freedom. SS: Sum of squares. MS: Mean square.

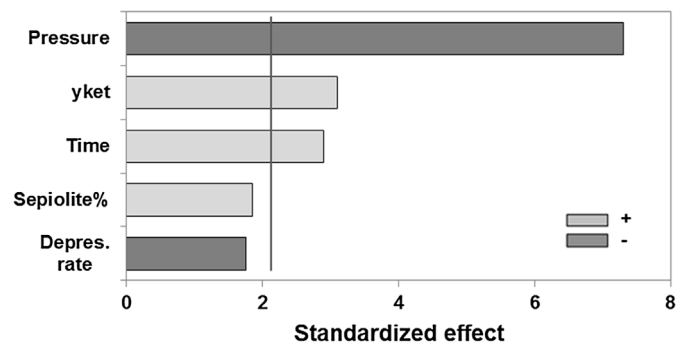


Fig. 6. Pareto diagram for impregnation yield (Y%) of ketones into sepiolite-LDPE nanocomposite films. A: sepiolite content; B: initial ketone mole fraction; C: pressure; D: depressurization rate; E: contact time.

is the highest, prevailing the effect of CO₂ sorption and polymer swelling at lower pressure, and the effect of CO₂ density (and solvent power) at higher values. For example, Li and Han [38] reported a maximum uptake of styrene in LDPE films at 13 MPa (at 35 °C) by scCO₂ impregnation. This behavior can also be inferred from the results of Torres et al. [16] and Rojas et al. [17], who observed an increase of solute loading from 7 to 12 MPa and a decrease from 12 to 22 MPa in the scCO₂ impregnation of LDPE films with thymol and 2-nonanone, respectively. Using a different type of polymer, Shen et al. [45] have reported a similar behavior in the case of cellulose acetate fibers impregnated with vanillin. In our case, results suggest that the effect of pressure (and CO₂ density) on the affinity of ketones towards the fluid phase is predominant in the range 9–13 MPa. This may be connected with the additional effect of pressure on the adsorption equilibrium of ketone solutes onto the sepiolite nanoparticles.

On the other hand, in the case of ketone mole fraction and contact time a significant positive effect was observed, indicating that these factors favor polymer impregnation. This result is consistent with the fact that the mole fraction of ketones in the fluid phase is the driving force for mass transfer into the polymer, and that diffusion inside the polymer is the rate-controlling step of the impregnation process. A similar enhancing effect of solute concentration and contact time on impregnation yield has been reported for example by Li and Han [38] when studying the impregnation of styrene into LDPE films with scCO₂ as solvent and swelling agent at 35 °C and 12 MPa. They observed that styrene uptake increased with both parameters until reaching a constant value, corresponding to polymer saturation. Similar impregnation kinetic curves have been measured and reported for other polymer-solute systems, such as synthetic dyes in polymethylmethacrylate (PMMA) [46] and thymol in cellulose acetate [20]. In our case, the

Table 4

Impregnation yield (Y %) obtained at the best process conditions ($P = 9$ MPa, $T = 45$ °C, depressurization rate = 0.5 MPa/min, time = 4 h), for films with different sepiolite content.

Sepiolite (%)	Impregnation yield (Y %) ^a
0	5.18 ± 0.20 ^a
1	8.54 ± 0.83 ^b
10	9.73 ± 0.32 ^b

Different letters indicate significant differences.

^a Mean values ± standard deviation with $n = 2$.

significant increase of ketone loading with contact time also suggests that the saturation of the films does not occur within the studied range, or at least at the lower level (2 h).

Although a certain increase on mean impregnation yield was observed as the sepiolite amount increased, as can be seen in Fig. 6, results indicate that there is no significant difference between using films with 1% and 10% sepiolite. This result will be discussed in the next section in connection with the morphological properties of the nanocomposite. Nevertheless, as it was mentioned above, in this work higher maximum values of impregnation yield were obtained compared to the ones observed in a previous work using pure LDPE films [25], although process conditions were not exactly the same. In order to confirm this enhancing effect of sepiolite on ketone loading yield under the same conditions, new impregnation experiments were performed under the best operation conditions determined in this work (corresponding to run 4) and using films with 10%, 1% and 0% sepiolite. The last one was obtained under the same conditions as the nanocomposite films but without the addition of sepiolite. The corresponding impregnation yield results are shown in Table 4. Results confirmed that, under these process conditions, the presence of sepiolite into the films enhanced the impregnation yield with respect to pure LDPE films, showing a significant difference according to ANOVA testing. Furthermore, the difference observed among the yield values for films with 1 and 10% sepiolite was not significant, which is in agreement with the results previously discussed, about the effect of the sepiolite content in the nanocomposite loading capacity.

3.2. Thermal and morphological analysis

Impregnated film samples (containing 1 and 10% sepiolite and processed at different pressure levels) were analyzed by DSC and compared with untreated films, in order to evaluate and gain insight about the effects of the impregnation process on the thermal properties and crystal morphology, as well as the role of the sepiolite nanofiller.

Table 5 shows the main thermal properties (melting temperatures, melting enthalpy and crystallinity degree) of selected treated and untreated samples. In Fig. 7, thermograms obtained by DSC for a 10% sepiolite film before and after impregnation at 9 and 13 MPa are shown. Three crystal populations with different melting range can be observed, characterized by the temperatures T_{m1} , T_{m2} and T_{m3} . It can be observed

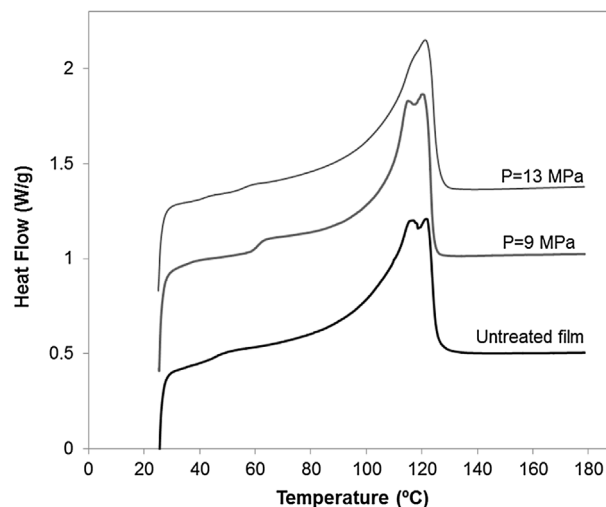


Fig. 7. DSC thermograms of untreated and impregnated LDPE/sepiolite nanocomposite films with 10% sepiolite. (Impregnation conditions: $T = 45$ °C; depressurization rate = 0.5 MPa/min; time = 4 h; initial ketone mole fraction = 0.0025).

that T_{m2} and T_{m3} correspond to long chain and highly ordered crystals of high melting point, while the small peak at T_{m1} indicates the presence of a minor portion of more disorganized crystals of shorter fold length. In turn, the occurrence of two main melting peaks is consistent with the structure proposed by other authors, consisting of a thick inner layer of crystals surrounding the particles (T_{m3}) and acting as nuclei for a secondary outer shell of thinner lamellae (T_{m2}) [47].

In a first place, it can be noticed that T_{m1} shifts from 50 to 55 °C in the original material to 60–65 °C after impregnation. At the process temperature (45 °C), the mobility of the polymer chains involved in this kind of crystals increases by the plasticizing effect induced by CO_2 sorption. Under these conditions, a reorganization in a more ordered arrangement (recrystallization), also enhanced by the nucleating effect of the nanofiller, is likely to occur, with a corresponding melting temperature increase. It is even possible that these crystals effectively melt and recrystallize at the operation temperature, considering that CO_2 sorption under high pressure conditions can induce a melting point depression, as observed for other semicrystalline polymers [48].

On the other hand, T_{m2} and T_{m3} are not affected in appreciable way by the impregnation process, remaining at or very close to their original values (114–117 and 121–122 °C, respectively). However, impregnation seems to reduce the relative amount of the T_{m2} population, effect more pronounced at higher pressure, as can be seen in Fig. 7 by comparing the thermograms of the samples impregnated at 9 and 13 MPa. This phenomenon can also be explained in terms of crystal reorganization induced by CO_2 sorption. The thicker and more perfect or long-folded crystals (T_{m3}), which are less affected by the plasticizing effect of CO_2 , act as nucleating agents and grow at the expense of the less perfect ones (T_{m2}). At higher pressure, CO_2 sorption increases and this phenomenon is enhanced. This CO_2 -induced recrystallization

Table 5

Thermal properties for original and impregnated LDPE/sepiolite nanocomposite films, processed at different impregnation pressure ($T = 45$ °C, depressurization rate = 0.5 MPa/min, time = 4 h).

Sepiolite (%)	Pressure (MPa)	T_{m1} (°C)	T_{m2} (°C)	T_{m3} (°C)	ΔH_m (J/g)	Crystallinity (%)
0	–	52.0	115.0	122.0	144.5	50.04
1	–	54.0	117.0	120.5	148.8	52.05
10	–	52.0	116.5	121.5	134.7	51.81
0	90	66.0	114.0	121.0	136.2	49.72
1	90	65.0	114.0	121.0	130.2	49.78
10	90	64.0	115.0	121.0	133.2	50.78
1	130	60.0	117.0	121.5	134.5	48.35
10	130	59.0	116.0	122.0	128.7	50.74

phenomenon has previously been observed and discussed by other authors in different polymeric systems [4,49–51], and some authors have postulated an analogy or compared it with the thermal recrystallization process or “annealing” [50,52].

The presence of sepiolite nanoparticles and their interactions with the polymeric matrix introduce further complexity to the sorption behavior of the composite (and therefore on its higher impregnation capacity) through different mechanisms. During film processing, the nanofiller particles act as nucleating agents, inducing crystallization from their surface in the form of lamellae rather than spherulites, which is the common crystallization mode of pure LDPE. However, a saturation effect is observed in the case of LDPE/sepiolite at around 1% of nanofiller, as crystallinity degree does not increase further with higher sepiolite concentrations. This phenomenon has been reported and discussed in a previous work [30], and can be observed in Table 5, where the films with 1 and 10% sepiolite show approximately the same crystallinity degree (~52%), slightly higher than the pure LDPE film (50%). This saturation effect implies that in the films with 1% sepiolite, there are less crystalline regions but with higher thickness around the nanoparticles, while in the films with 10% sepiolite the crystalline lamellae are more numerous and distributed, but thinner. In fact, a previous characterization of the films by atomic force microscopy (AFM) [30] allowed to estimate the lamellar thickness, showing a decrease from approx. 40 nm in the films with 1% sepiolite to 20 nm in the films with 10% sepiolite. Additionally, DSC analysis of pure LDPE and nanocomposites films shows an increase in the T_{m2}/T_{m3} populations relative ratio with the sepiolite content, as can be seen in Fig. 8.

On the other hand, XRD analysis revealed some differences in LDPE crystal morphology when sepiolite was incorporated, which depended on the sepiolite content. As mentioned, this analysis was carried out placing the samples with film stretching direction parallel and perpendicular to the beam, in order to detect differences in crystal morphology with the flow direction during film extrusion and casting process. In Fig. 9, XRD patterns obtained for nanocomposite films prepared with 1% and 10% sepiolite in both directions are shown. It can be observed that sepiolite favors LDPE crystallization in monoclinic phase, in perpendicular direction to the film flow, as indicated by the appearance of two typical peaks of that phase (13.8° and 16.7°), in addition to the characteristic peaks of orthorhombic crystal phase (21.3° and 36.5°) observed for pure LDPE. Besides, a higher orientation of orthorhombic crystals when increasing the nanofiller content was detected, which may be promoted by the flow-induced orientation of the acicular sepiolite particles [30]. The crystal orientation induces a channeling phenomenon, establishing preferential paths within the polymeric matrix for scCO_2 and ketone molecules diffusion [53], making amorphous regions more easily accessible to penetrating solutes

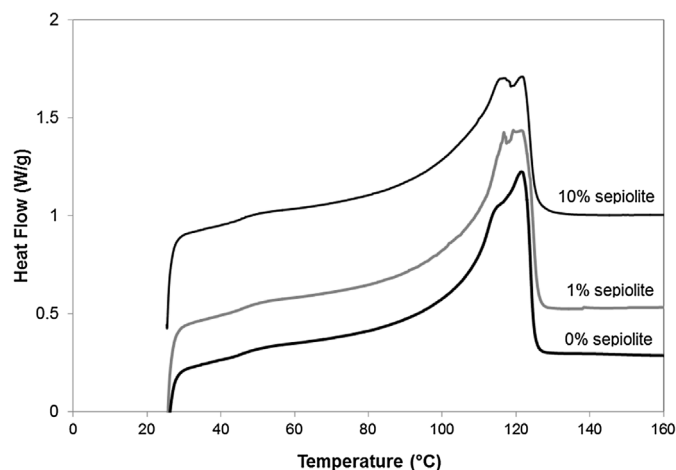


Fig. 8. DSC thermograms of untreated LDPE and LDPE/sepiolite nanocomposite films.

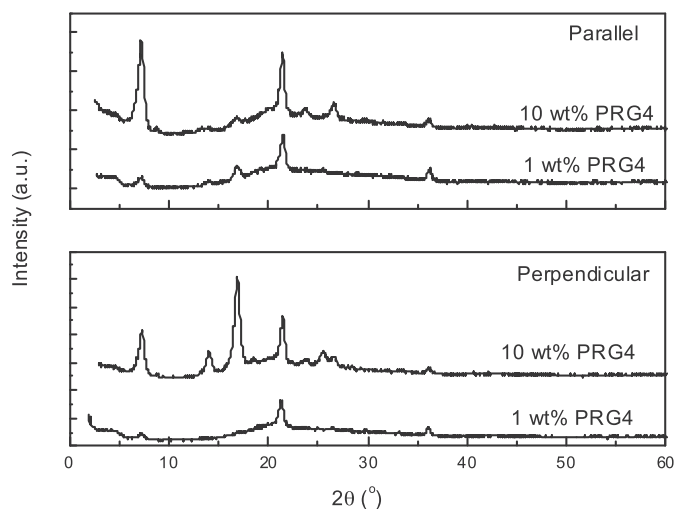


Fig. 9. XRD diffraction patterns obtained for nanocomposite films prepared with 1 and 10% (w/w) of sepiolite, in both directions (parallel and perpendicular to the X-ray beam).

by reducing the tortuosity.

It is also important to remark that acicular particles induce transcrystallinity around them [30], with crystals growing from their surface due to nucleation effect. This phenomenon could impede the ketone penetration into the sepiolite particles, considering that the crystalline layers act as a practically impermeable obstacles to diffusing molecules. However, crystals are always separated by amorphous domains, which allows the active substances to interpenetrate among crystals nucleated on the sepiolite surface and then be adsorbed by the filler. The hindrance effect is higher in the nanocomposites with 1% sepiolite where the lamellae thickness is higher, while nanocomposite films prepared with 10% sepiolite present thinner crystals around the particles which allow a higher ketone penetration through the interconnecting amorphous zones. These thinner crystalline domains are also more easily plasticized by scCO_2 during impregnation, enhancing the overall diffusional properties of the film.

Besides these phenomena, it is well-known that crystalline domains restrict the mobility of the polymeric chains, limiting the swelling capacity and the free volume available for solute diffusion in the amorphous regions. Thus, sepiolite particles act as anchor points, as well as nucleating agents. According to the crystal morphology described above, in nanocomposite films with 1% sepiolite, there are less amorphous domains but with higher size, while with 10% sepiolite the size of the amorphous zones decreases but they are more distributed between crystals growing from the nanoparticles surface. For this reason, the amorphous zones in the films with higher amount of sepiolite have lower swelling capability and therefore lower sorption capacity.

In summary, the presence of sepiolite nanoparticles and their interaction with the polymeric matrix have three main effects which are specially relevant for the impregnation process: (a) different crystal morphology and distribution, depending on sepiolite content: less but thicker crystalline domains at 1% sepiolite, and thinner but more numerous (and more easily plasticized) crystals at 10% sepiolite; (b) an oriented microstructure, which facilitates diffusion in the amorphous regions by a channeling phenomenon; (c) mechanical restrictions to polymer swelling, which are unfavorable for impregnation yield and increase with sepiolite content. The interplay of these effects, added to the intrinsic adsorption capacity of the nanoparticles (more or less hindered by the crystal layers around them), may explain the fact that maximum impregnation yield in LDPE/sepiolite nanocomposite films is higher than in pure LDPE films, as well as the observation that the increase in sepiolite concentration does not contribute significantly to further enhance impregnation yield. In this sense, adsorption-desorption equilibrium tests using ketones and pure sepiolite under scCO_2

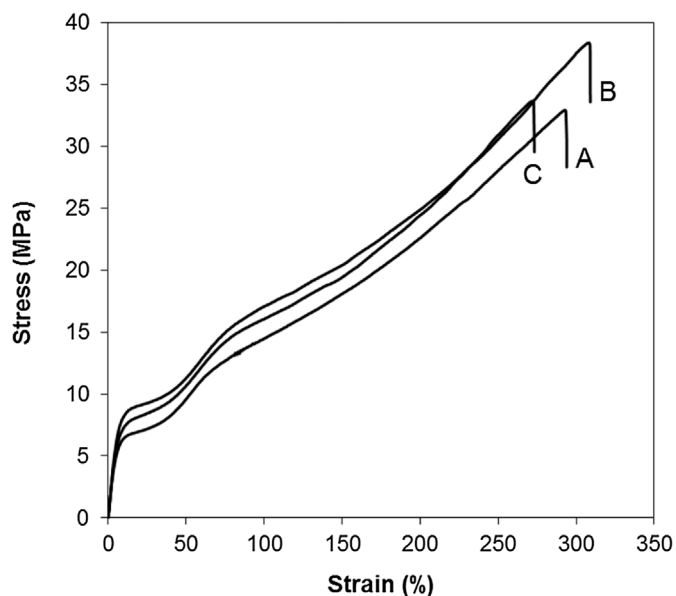


Fig. 10. Stress-strain curves for LDPE/sepiolite films. A: untreated; B: pressurized; C: impregnated (run 4).

conditions could provide deeper insight of this mechanism, as well as quantitative information, keeping in mind that sepiolite particles in the nanocomposite are partially covered by LDPE crystals, and therefore their surface is not fully available to adsorb solute molecules.

3.3. Mechanical properties

Typical stress-strain curves for ketone-impregnated, pressurized with pure scCO_2 and untreated films are shown in Fig. 10. In the case of impregnated films, only the samples with higher ketone yield (corresponding to run 4) were tested. The pressurized films, treated under the same conditions but without addition of ketones, were tested in order to evaluate separately the effect of the scCO_2 processing and the incorporation of ketones.

The curves show the typical behavior of oriented ductile materials when stretched in the orientation direction. It can be seen that strain hardening begins immediately after yielding, and elongation increases up to $\sim 300\%$ before break.

The mean values of the main mechanical properties (Young modulus, elongation at break, yield and tensile strength) are reported in Table 6. As can be seen, the tensile strength and elongation at break were practically not affected by the high pressure treatment nor the incorporation of ketones. The Young modulus showed an increase after treatments, which was about 34% for the pressurized samples and about 16% for the ketone impregnated films. This means that the pressurization under pure scCO_2 induces a stiffening of the material, which is partially counterbalanced by the plasticizing effect due to the incorporation of ketones. The yield strength followed a similar behavior.

Therefore, it can be concluded that the high pressure impregnation process did not affect the material ductility and tensile strength, while it increased to some degree the stress required for plastic deformation. These effects can be related to the previously discussed changes in the

polymer morphology, as observed in the DSC analysis. In fact, the melting temperature T_{m1} , corresponding to imperfect and short chain crystals, shifted from 45 to 50 °C in the original films to 65–70 °C after impregnation. This new population of crystals of higher melting temperature (indicating a higher organization degree) may explain the observed stiffening of the films within the elastic region after treatment. The previously discussed growing of highly ordered crystals at the expense of less organized ones (T_{m3} vs. T_{m2}), although limited, may also contribute to this phenomenon.

In a previous work concerning the scCO_2 -assisted impregnation of LDPE films with eugenol [18], a decrease in Young modulus, yield strength and elongation was observed after impregnation and scCO_2 pressurization, with a markedly different stress-strain behavior. Those effects were attributed to a net loss of crystallinity due to the plasticizing effect of CO_2 and eugenol. In the present case, the presence of sepiolite particles seems to “stabilize” the polymer structure, also inducing a higher recrystallization, as previously discussed. Thus, the films practically recovered their original crystallinity degree after treatment (with some morphological modifications), with a very low impact on their mechanical performance.

4. Conclusions

In this work, the incorporation of two terpene ketones with insecticidal activity into LDPE/sepiolite nanocomposite film using scCO_2 -assisted impregnation was explored as a strategy to enhance loading yield with respect to pure LDPE. The statistical analysis of the results indicated that the impregnation pressure, the initial mole fraction of ketones in the fluid phase and the contact time are the process parameters which affect significantly the impregnation yield. The observed increase in impregnation yield could be explained in terms of the effects of high pressure CO_2 sorption by the polymeric matrix and the changes in the crystal morphology and diffusional properties of the films induced by this phenomenon as well as the presence of the sepiolite nanoparticles. Among the 16 different experimental conditions tested, best results were obtained operating at 9 MPa, with an initial ketone mole fraction $y = 0.0025$ and 4 h of contact time, with a depressurization rate of 0.5 MPa/min (low) and using films with 10% sepiolite, corresponding to an impregnation yield of $8.60 \pm 1.66\%$ (w/w). However, as depressurization rate and sepiolite content seem not to have a significant effect on yield, these factors can be considered as “degrees of freedom” which can be set at the most convenient levels regarding other process aspects (related to economic issues, energy consumption or technological requirements). In sum, the screening analysis here reported provides useful information for a finer tuning of the operation conditions as well as for the impregnation process optimization. Finally, tensile strength tests showed that the incorporation of sepiolite into the polymeric matrix preserved the main mechanical properties of the films.

Acknowledgments

The authors acknowledge the financial support of Universidad Nacional de Córdoba (UNC, Argentina. Proyecto SECyT 2015) and Agencia Nacional de Promoción Científica y Tecnológica (ANPCyT, Argentina. PICT Startup 2011-0726). M.L. Goñi gratefully acknowledges Consejo Nacional de Investigaciones Científicas y Técnicas

Table 6
Mechanical properties of untreated, pressurized and impregnated LDPE/sepiolite films (run 4).

Sample	Young modulus (MPa)	Yield strength (MPa)	Tensile strength (MPa)	Elongation at break (%)
(A) Untreated films	108.40 \pm 17.02	6.99 \pm 0.72	33.07 \pm 1.61	320.25 \pm 40.73
(B) Pressurized films	145.87 \pm 7.06	8.04 \pm 1.55	30.21 \pm 7.27	315.33 \pm 28.04
(C) Impregnated films	125.10 \pm 37.36	7.32 \pm 0.84	33.03 \pm 1.81	324.75 \pm 64.92

(CONICET, Argentina) for her postdoctoral fellowship. N.A. Gañán, S.E. Barbosa, M.C. Strumia and R.E. Martini are career members of CONICET (Argentina).

References

- [1] S.G. Kazarian, Polymer processing with supercritical fluids, *Polym. Sci.* 42 (2000) 78–101, <http://dx.doi.org/10.1080/03602549909351647>.
- [2] E. Kiran, Supercritical fluids and polymers – The year in review – 2014, *J. Supercrit. Fluids* 110 (2016) 126–153, <http://dx.doi.org/10.1016/j.supflu.2015.11.011>.
- [3] I. Kikic, F. Vecchione, Supercritical impregnation of polymers, *Curr. Opin. Solid State Mater. Sci.* 7 (2003) 399–405, <http://dx.doi.org/10.1016/j.cossms.2003.09.001>.
- [4] D.L. Tomasko, H.B. Li, D.H. Liu, X.M. Han, M.J. Wingert, L.J. Lee, et al., A review of CO₂ applications in the processing of polymers, *Ind. Eng. Chem. Res.* 42 (2003) 6431–6456, <http://dx.doi.org/10.1021/ie030199z>.
- [5] Y.-T. Shieh, J.-H. Su, G. Manivannan, P.H.C. Lee, S.P. Sawan, W.D. Spall, Interaction of supercritical carbon dioxide with polymers. I. Crystalline polymers, *J. Appl. Polym. Sci.* 59 (1996) 695–705.
- [6] Y.-T. Shieh, J.-H. Su, G. Manivannan, P.H.C. Lee, S.P. Sawan, W.D. Spall, Interaction of supercritical carbon dioxide with polymers. II. Amorphous polymers, *J. Appl. Polym. Sci.* 59 (1996) 707–717, [http://dx.doi.org/10.1002/\(SICI\)1097-4628\(19960124\)59:4<707::AID-APP16>3.0.CO;2-M](http://dx.doi.org/10.1002/(SICI)1097-4628(19960124)59:4<707::AID-APP16>3.0.CO;2-M).
- [7] M. Pantoula, C. Panayiotou, Sorption and swelling in glassy polymer/carbon dioxide systems. Part I-Sorption, *J. Supercrit. Fluids* 37 (2006) 254–262.
- [8] M. Pantoula, J. von Schnitzler, R. Eggers, C. Panayiotou, Sorption and swelling in glassy polymer/carbon dioxide systems. Part II-Swelling, *J. Supercrit. Fluids* 39 (2007) 426–434, <http://dx.doi.org/10.1016/j.supflu.2006.03.010>.
- [9] I. Kikic, F. Vecchione, P. Alessi, A. Cortesi, F. Eva, N. Elvassore, Polymer plasticization using supercritical carbon dioxide: experiment and modeling, *Ind. Eng. Chem. Res.* 42 (2003) 3022–3029, <http://dx.doi.org/10.1021/ie020961h>.
- [10] I. Kikic, Polymer-supercritical fluid interactions, *J. Supercrit. Fluids* 47 (2009) 458–465, <http://dx.doi.org/10.1016/j.supflu.2008.10.016>.
- [11] E. Bach, E. Cleve, E. Schollmeyer, Past, present and future of supercritical fluid dyeing technology – an overview, *Rev. Prog. Color. Relat. Top.* 32 (2002) 88–102.
- [12] M. Bancho, Supercritical fluid dyeing of synthetic and natural textiles – a review, *Color. Technol.* 129 (2013) 2–17.
- [13] V.P. Costa, M.E.M. Braga, J.P. Guerra, A.R.C. Duarte, C.M.M. Duarte, E.O.B. Leite, et al., Development of therapeutic contact lenses using a supercritical solvent impregnation method, *J. Supercrit. Fluids* 52 (2010) 306–316, <http://dx.doi.org/10.1016/j.supflu.2010.02.001>.
- [14] M. Champeau, J.-M. Thomassin, T. Tassaing, C. Jerome, Drug loading of sutures by supercritical CO₂ impregnation: effect of polymer/drug interactions and thermal transitions, *Macromol. Mater. Eng.* 300 (2015) 596–610, <http://dx.doi.org/10.1002/mame.201400369>.
- [15] M. Champeau, J.-M. Thomassin, T. Tassaing, C. Jérôme, Drug loading of polymer implants by supercritical CO₂ assisted impregnation: a review, *J. Control. Release* 209 (2015) 248–259, <http://dx.doi.org/10.1016/j.jconrel.2015.05.002>.
- [16] A. Torres, J. Romero, A. Macan, A. Guarda, M.J. Galotto, Near critical and supercritical impregnation and kinetic release of thymol in LLDPE films used for food packaging, *J. Supercrit. Fluids* 85 (2014) 41–48, <http://dx.doi.org/10.1016/j.supflu.2013.10.011>.
- [17] A. Rojas, D. Cerro, A. Torres, M.J. Galotto, A. Guarda, J. Romero, Supercritical impregnation and kinetic release of 2-nonanone in LLDPE films used for active food packaging, *J. Supercrit. Fluids* 104 (2015) 76–84, <http://dx.doi.org/10.1016/j.supflu.2013.10.011>.
- [18] M.L. Goñi, N.A. Gañán, M.C. Strumia, R.E. Martini, Eugenol-loaded LLDPE films with antioxidant activity by supercritical carbon dioxide impregnation, *J. Supercrit. Fluids* 111 (2016) 28–35, <http://dx.doi.org/10.1016/j.supflu.2016.01.012>.
- [19] A.C. De Souza, A.M. a Dias, H.C. Sousa, C.C. Tadini, Impregnation of cinnamaldehyde into cassava starch biocomposite films using supercritical fluid technology for the development of food active packaging, *Carbohydr. Polym.* 102 (2014) 830–837, <http://dx.doi.org/10.1016/j.carbpol.2013.10.082>.
- [20] S. Milovanovic, M. Stamenic, D. Markovic, I. Ivanovic, I. Zizovic, Supercritical impregnation of cellulose acetate with thymol, *J. Supercrit. Fluids* 97 (2015) 107–115, <http://dx.doi.org/10.1016/j.supflu.2014.11.011>.
- [21] A. Torres, E. Ilabaca, A. Rojas, F. Rodríguez, M.J. Galotto, A. Guarda, et al., Effect of processing conditions on the physical, chemical and transport properties of poly-lactic acid films containing thymol incorporated by supercritical impregnation, *Eur. Polym. J.* 89 (2017) 195–210, <http://dx.doi.org/10.1016/j.eurpolymj.2017.01.019>.
- [22] J. Fernandes, A.W. Kjellow, O. Henriksen, Modeling and optimization of the supercritical wood impregnation process – Focus on pressure and temperature, *J. Supercrit. Fluids* 66 (2012) 307–314, <http://dx.doi.org/10.1016/j.supflu.2012.03.003>.
- [23] S.B. Iversen, T. Larsen, O. Henriksen, K. Felsvang, *The World's First Commercial Supercritical Wood Treatment Plant*, 6th Int Symp. Supercrit. Fluids, ISASF, Versailles, 2003.
- [24] H. Zheng, J. Zhang, J. Yan, L. Zheng, An industrial scale multiple supercritical carbon dioxide apparatus and its eco-friendly dyeing production, *J. CO₂ Util.* 16 (2016) 272–281, <http://dx.doi.org/10.1016/j.jcou.2016.08.002>.
- [25] M.L. Goñi, N.A. Gañán, J.M. Herrera, M.C. Strumia, A.E. Andreatta, R.E. Martini, Supercritical CO₂ of LDPE films with terpene ketones as pesticides against corn weevil (*Sitophilus zeamais*), *J. Supercrit. Fluids* 122 (2017) 18–26, <http://dx.doi.org/10.1016/j.supflu.2016.11.017>.
- [26] J.M. Herrera, M.P. Zunino, J.S. Dambolena, R.P. Pizzolitto, N.A. Gañán, E.I. Lucini, et al., Terpene ketones as natural insecticides against *Sitophilus zeamais*, *Ind. Crops Prod.* 70 (2015) 435–442, <http://dx.doi.org/10.1016/j.indcrop.2015.03.074>.
- [27] J.M. Herrera, M.L. Goñi, N.A. Gañán, J.A. Zygadlo, An insecticide formulation of terpene ketones against *Sitophilus zeamais* and its incorporation into low density polyethylene films, *Crop Prot.* 98 (2017) 33–39, <http://dx.doi.org/10.1016/j.cropro.2017.03.008>.
- [28] S.D.F. Mihindukulasuriya, L.T. Lim, Nanotechnology development in food packaging: a review, *Trends Food Sci. Technol.* 40 (2014) 149–167, <http://dx.doi.org/10.1016/j.tifs.2014.09.009>.
- [29] B. Casal, J. Merino, J.M. Serratos, E. Ruiz-Hitzky, Sepiolite-based materials for the photo- and thermal-stabilization of pesticides, *Appl. Clay Sci.* 18 (2001) 245–254, [http://dx.doi.org/10.1016/S0169-1317\(01\)00030-8](http://dx.doi.org/10.1016/S0169-1317(01)00030-8).
- [30] R.E. Martini, S. La Tegola, A. Terenzi, J.M. Kenny, S.E. Barbosa, Polyethylene-based nanocomposite films: structure/properties relationship, *Polym. Eng. Sci.* 54 (2014) 1931–1940, <http://dx.doi.org/10.1002/pen.23743>.
- [31] E. Galan, Properties and applications of Palygorskite-sepiolite clays, *Clay Miner.* 31 (1996) 443–453.
- [32] F. Tornuk, M. Hancer, O. Sagdic, H. Yetim, LLDPE based food packaging incorporated with nanoclays grafted with bioactive compounds to extend shelf life of some meat products, *LWT – Food Sci. Technol.* 64 (2015) 540–546, <http://dx.doi.org/10.1016/j.lwt.2015.06.030>.
- [33] B. Giménez, M.C. Gómez-Guillén, M.E. López-Caballero, J. Gómez-Estaca, P. Montero, Role of sepiolite in the release of active compounds from gelatin-egg white films, *Food Hydrocoll.* 27 (2012) 475–486, <http://dx.doi.org/10.1016/j.foodhyd.2011.09.003>.
- [34] A. Chevillard, H. Angellier-Coussy, V. Guillard, N. Gontard, E. Gastaldi, Controlling pesticide release via structuring agropolymer and nanoclays based materials, *J. Hazard. Mater.* 205–206 (2012) 32–39, <http://dx.doi.org/10.1016/j.jhazmat.2011.11.093>.
- [35] D.C. Montgomery, *Design and Analysis of Experiments*, 8th ed., John Wiley & Sons, Inc., Hoboken, NJ/USA, 2013.
- [36] M.J. Anderson, P.J. Whitcomb, DOE, Simplified, CRC, Press, Boca Raton, USA, 2007.
- [37] J. Haslam, H.A. Willis, D.C.M. Squirrel, *Identification and Analysis of Plastics*, 2nd ed., Iliffe Books, London, 1972.
- [38] D. Li, B. Han, Impregnation of polyethylene (PE) with styrene using supercritical CO₂ as the swelling agent and preparation of PE/Polystyrene composites, *Ind. Eng. Chem. Res.* 39 (2000) 4506–4509, <http://dx.doi.org/10.1021/ie000228v>.
- [39] T. Perraki, A. Orfanoudaki, Study of raw and thermally treated sepiolite from the Mantoudi area, Euboea, Greece: x-ray diffraction, TG/DTG/DTA and FTIR investigations, *J. Therm. Anal. Calorim.* 91 (2008) 589–593, <http://dx.doi.org/10.1007/s10973-007-8329-8>.
- [40] A.B. Raschi, E. Romano, A.M. Benavente, A. Ben Altabel, M.E. Tuttolomondo, Structural and vibrational analysis of thymoquinone, *Spectrochim. Acta – Part A Mol. Biomol. Spectrosc.* 77 (2010) 497–505, <http://dx.doi.org/10.1016/j.saa.2010.06.026>.
- [41] E.A. Petrakis, A.C. Kimbaris, C.S. Pappas, P.A. Tarantilis, M.G. Polissiou, Quantitative determination of pulegone in pennyroyal leaf by FT-IR spectroscopy, *J. Agric. Food Chem.* 57 (2009) 10044–10048, <http://dx.doi.org/10.1021/jf9026052>.
- [42] R.G. Wissing, M.E. Paulaitis, Swelling and sorption in polymer-CO₂ mixtures at elevated pressures, *J. Polym. Sci. Part B Polym. Phys.* 25 (1987) 2497–2510.
- [43] G. Brunner, M. Johannsen, New aspects on adsorption from supercritical fluid phases, *J. Supercrit. Fluids* 38 (2006) 181–200, <http://dx.doi.org/10.1016/j.supflu.2006.06.008>.
- [44] M. Sato, M. Kondo, M. Goto, A. Kodama, T. Hirose, Fractionation of citrus oil by supercritical countercurrent extractor with side-stream withdrawal, *J. Supercrit. Fluids* 13 (1998) 311–317.
- [45] Z. Shen, G.S. Huvar, C.S. Warriner, M. Mc Hugh, J.L. Banyasz, M.K. Mishra, CO₂-assisted fiber impregnation, *Polymer (Guildf)* 49 (2008) 1579–1586, <http://dx.doi.org/10.1016/j.polymer.2008.01.020>.
- [46] S.G. Kazarian, N.H. Brantley, B.L. West, M.F. Vincent, C.A. Eckert, In situ spectroscopy of polymers subjected to supercritical CO₂: Plasticization and dye impregnation, *Appl. Spectrosc.* 51 (1997) 491–494, <http://dx.doi.org/10.1366/0003702971940765>.
- [47] C. Frederix, J.M. Lefebvre, C. Rochas, R. Séguéla, G. Stoclet, Binary blends of linear ethylene copolymers over a wide crystallinity range: rheology, crystallization, melting and structure properties, *Polymer (Guildf)* 51 (2010) 2903–2917, <http://dx.doi.org/10.1016/j.polymer.2010.04.045>.
- [48] Z. Zhang, Y.P. Handa, CO₂-assisted melting of semicrystalline polymers, *Macromolecules* 30 (1997) 8505–8507, <http://dx.doi.org/10.1021/ma9712211>.
- [49] E. Kiran, K. Liu, K. Ramsdell, Morphological changes in poly(ϵ -caprolactone) in dense carbon dioxide, *Polymer (Guildf)* 49 (2008) 1853–1859, <http://dx.doi.org/10.1016/j.polymer.2008.02.017>.
- [50] G. Mensitieri, M.A. Del Nobile, G. Guerra, A. Apicella, H. Al Ghatta, Crystallized modified PETS, *Polym. Eng. Sci.* 35 (1995) 506–512.
- [51] S.M. Lambert, M.E. Paulaitis, Crystallization of poly(ethylene terephthalate) induced by carbon dioxide sorption at elevated pressures, *J. Supercrit. Fluids* 4 (1991) 15–23, [http://dx.doi.org/10.1016/0896-8446\(91\)90026-3](http://dx.doi.org/10.1016/0896-8446(91)90026-3).
- [52] H. Sun, R.S. Cooke, W.D. Bates, K.J. Wynne, Supercritical CO₂ processing and annealing of polytetrafluoroethylene (PTFE) and modified PTFE for enhancement of crystallinity and creep resistance, *Polymer (Guildf)* 46 (2005) 8872–8882, <http://dx.doi.org/10.1016/j.polymer.2005.05.134>.
- [53] Y.N. Alonso, A.L. Grafia, L.A. Castillo, S.E. Barbosa, Lemon essential oil desorption from polypropylene/talc nanocomposite films, *Iran. Polym. J.* 25 (2016) 999–1008, <http://dx.doi.org/10.1007/s13726-016-0485-x>.